Microchemical Journal 216 (2025) 114769

Contents lists available at ScienceDirect

Microchemical Journal

journal homepage: www.elsevier.com/locate/microc

Composite material based on ZIF-8, reduced graphene oxide, and Nafion as electrode modifier for dopamine electrooxidation

Alexandra Belcovici [a], Davide Tocco [c], Emiliano Fratini [c], Andrea Salis [b,*], Graziella Liana Turdean [a,*]

[a] "Babeş-Bolyai" University, Faculty of Chemistry and Chemical Engineering, Department of Chemical Engineering, Research Centre of Electrochemistry and Non-Conventional Materials, 11 Arany Janos St., RO-400028 Cluj-Napoca, Romania
[b] Università degli Studi di Cagliari & CSGI, Dipartimento di Scienze Chimiche e Geologiche, Cittadella Universitaria SS 554 bivio Sestu, 09042 Monserrato, Cagliari, Italy
[c] University of Florence & CSGI, Department of Chemistry "Ugo Schiff", via della Lastruccia 3, Sesto Fiorentino (FI) I-50019, Italy

ARTICLE INFO

Keywords:
ZIF-8
Metal-organic frameworks
Reduced graphene oxide
Nanocomposite
Chemically modified electrode
Dopamine

ABSTRACT

A zeolitic imidazolate framework (ZIF-8), a subclass of metal-organic frameworks (MOFs) was synthesised and morpho-structural characterised by X-ray diffraction (XRD), thermogravimetric analysis (TGA), FT-IR and Raman spectroscopy, N_2 adsorption/desorption isotherms and scanning electron microscopy (SEM). A ZIF-8–rGO–Nafion/GCE modified electrode was prepared by the drop-casting method from a solution containing reduced graphene oxide (rGO), ZIF-8 and Nafion. The modified electrode was characterised by cyclic voltammetry (CV), electrochemical impedance spectroscopy (EIS) and square-wave voltammetry (SWV) for dopamine (DA) detection. The influence of scan rate and pH (by CV), corroborated with EIS data, led to estimating different electrochemical parameters of the dopamine oxidation process. By SWV, ZIF-8–rGO–Nafion/GCE modified electrode showed good analytical performances, such as: linear domain 0.5–1.4 μM, limit of detection of 0.051 μM dopamine when alone, and 0.069 μM dopamine in the simultaneous detection with paracetamol and citric acid, good electrode stability (RSD 7.43 %) and reproducibility (RSD 1.72 %), expressed for peak current intensities. A standard addition method applied to DA samples led to recovery values ranging from 110.8 % to 112.6 %, proving the reliability of the ZIF-8–rGO–Nafion/GCE modified electrode to be used in the analysis of real samples.

1. Introduction

Metal-Organic Frameworks (MOFs) are a class of porous materials constituted by a metal node/cluster and an organic ligand linked through coordination bonds [1]. They have a modular structure, which offers enormous structural diversity and wide possibilities for creating materials with tailored properties. MOFs can be synthesised using different approaches, both traditional and rather specific ones, such as microwave, ultrasonic, mechanochemical, and electrochemical processing [2]. Due to their properties, MOFs are suitable for several applications, such as gas adsorption [3], catalysis [4], sensing [5], drug delivery [6], removal of pollutants from water [7,8], enzyme immobilization [9,10], and other industrial applications [11].

In particular, zeolitic imidazolate frameworks (ZIFs), are a class of MOFs formed by the coordination of Zn^{2+} or Co^{2+} with imidazole-type linkers [12]. Since the metal-imidazole-metal angle is similar to that of Si-O-Si (145°) in zeolites, ZIFs are topologically isomorphic with zeolites [13]. The strong interaction between the charged imidazolate linkers and the metal ions and the formation of rigid cages make ZIFs highly robust porous materials. Among the ZIFs subclass, ZIF-8 has good thermal stability (up to 350 °C), and tuneable porosity. Moreover, ZIF-8 samples typically show higher surface areas in comparison with zeolites [14,15]. ZIF-8 forms crystals with rhombic dodecahedral morphology and sodalite (sod) topology. ZIFs combine highly desirable properties of zeolites and MOFs and have emerged as a versatile type of crystalline porous material. Functional applications of ZIFs in separation, catalysis, sensing and energy storage fields have been reported in the past few years. Compared with common MOFs, ZIFs with stable structures can be prepared easily under mild conditions, like ambient temperature and atmospheric pressure in methanol, or even in aqueous solutions [16].

Reduced graphene oxide (rGO) – obtained from graphene oxide (GO) by electro/chemical reduction, thermal decomposition, and other

* Corresponding authors.
E-mail addresses: asalis@unica.it (A. Salis), graziella.turdean@ubbcluj.ro (G.L. Turdean).

https://doi.org/10.1016/j.microc.2025.114769
Received 28 December 2024; Received in revised form 25 July 2025; Accepted 1 August 2025
Available online 5 August 2025

methods (e.g., microwave, photolytic, or radiation treatment), or their combination - is a promising graphene derivative that attracts attention due to its unique properties [17,18]. rGO maintains the morphology, and the structural or functional properties of the precursor, with enhanced values (i.e., high specific surface area, low oxygen content, and good electric conductivity). Also, by controlling the number of remaining functional groups during the synthesis process, it is relatively easy to control the enhancement of the electrical performance and solubility of rGO [18,19]. Consequently, rGO is used in many chemical and biological applications, such as adsorbents, catalysts, sensing elements, energy storage (e.g., solar cells), and conversion technologies [17,19].

Thus, the introduction of rGO in the electrode modifier matrix accelerates the electron transfer between the composites matrix and the supporting electrode surface improving the electrochemical detection sensitivity. Also, it was reported in the literature that the synergistic effect of graphene and ZIF-8, leads to obtaining a fast mass transfer and higher electrical conductivity [20].

Nafion is a conductive sulfonated tetrafluoroethylene-based fluoropolymer–copolymer, used as an electrode modifier due to its excellent film-forming ability. Nafion is a highly hydrophobic matrix that effectively disperses graphene derivatives in an aqueous solution because of the perfluoroalkyl groups it contains. Additionally, the presence of negatively charged groups in Nafion favours the attraction of positively charged compounds (dopamine at pH 7), thus accelerating the electron transfer process in graphene derivatives [21].

Dopamine (DA) plays an important role as a neurotransmitter in the mammalian central nervous system (CNS) and is also a key factor in the function of renal and cardiovascular systems. The concentration of DA in biological systems usually ranges from 10^{-8} M to 10^{-6} M, abnormal levels or practically complete depletion of DA in the CNS are related to neurological diseases (e.g., Parkinson's disease). Therefore, the selective and sensitive detection of DA in biological systems is of great clinical importance for correct diagnosis. Classical methods for DA quantitative analysis include liquid chromatography, capillary electrophoresis, chemiluminescence and colorimetry [20], that have many drawbacks, such as expensiveness, bulky volume, requirement of highly skilled personnel, and time-consuming and/or sophisticated pretreatment processes (e.g., preconcentration step and/or micro/extraction). In order to overcome the abovementioned disadvantages, electrochemical techniques based on chemically modified electrodes offer a promising alternative to the previously mentioned conventional methods. Thus, the development of rapid, real-time, and highly selective dopamine determination by electroanalytical methods is facilitated by the chemically modified electrodes' key properties, which include high sensitivity, fast response time, simplicity, low cost, and in situ detection capacity [4,22]. Until now, various types of electrode matrix, including nanostructured carbon [23], metal nanoparticles [23], metal oxides [23], conducting polymers [23], and enzymes (i.e., tyrosinase or laccase) [24] have been studied to improve dopamine sensing performance [23]. The benefits of combining ZIF and graphene include a large internal surface area, adjustable and tuneable porous structures, numerous functional groups for superior adsorption ability, open active metal sites for rich redox catalysis (in the case of ZIF), and simple chemical modification options for selective sensing. As far as we know, before being deposited on an electrode surface, the previously published studies employed various materials obtained in a chemical process between graphene or graphene oxide materials and ZIF compounds [22,25]. Contrarily, this work used an easy procedure that involved mixing ZIF-8 material with rGO and Nafion solution to produce a composite mixture. The obtained suspension was then dropped onto a glassy carbon electrode (ZIF-8–rGO–Nafion/GCE) and used to detect dopamine. The synergistic effect of the high conductivity of the reduced graphene oxide (rGO) and the high electroactive surface area of the obtained composite electrode matrix was investigated by cyclic voltammetry and electrochemical impedance spectroscopy. Moreover, some analytical parameters (i.e., limit of detection and sensitivity) were also estimated using square-wave voltammetry.

2. Experimental

2.1. Reagents

The reagents used in this study are: zinc nitrate hexahydrate (98 %, from Sigma-Aldrich, Milan, Italy), 2-methylimidazole (99 %, purchased from Sigma-Aldrich, Milan, Italy), reduced graphene oxide (rGO, from Graphenea, Spain), Nafion 5 % ethanolic solution (from Sigma Aldrich), Na_2HPO_4, NaH_2PO_4 (from Sigma Aldrich), dopamine hydrochloride (Sigma Aldrich), paracetamol (Sun Pharma, "Terapia", Romania), citric acid (Sigma Aldrich), glucose (Sigma Aldrich), $K_4[Fe(CN)_6]$, $K_3[Fe(CN)_6]$ and NaCl, KCl ("Reactivul" Bucuresti, Romania). A 0.1 M phosphate buffer (PB) solution (at pH 7) was prepared by dissolving appropriate weights of Na_2HPO_4 and NaH_2PO_4 salts (from "Reactivul" Bucuresti). The 1×10^{-4} M dopamine solution was prepared in PB solution, prior to use. All chemicals were of analytical grade (i.e., puriss. p. a.) and used as received. Dopamine vials (5 mg/mL dopamine hydrochloride, produced by Zentiva) were purchased from a local pharmacy.

2.2. Methods

Electrochemical experiments (cyclic voltammetry, square wave voltammetry, and electrochemical impedance spectroscopy) were carried out using an AUTOLAB potentiostat (model PGSTAT 302N and PGSTAT 12, Metrohm, Netherlands) connected to a conventional three-electrode set-up equipped with a ZIF-8-rGO-Nafion/GCE working electrode, a Pt wire as auxiliary electrode, and an Ag/AgCl as reference electrode. The electrochemical investigation of dopamine, paracetamol and citric acid by square wave anodic stripping voltammetry (SWAS*V*) was performed in the potential range from −0.4 to 0.7 V vs. Ag/AgCl, KCl_{sat}. Electrochemical impedance spectra were recorded in a frequency range of 10^{-1}–10^{4} Hz using ZIF-8–rGO–Nafion/GCE modified electrode immersed in a 0.1 M KCl containing 5 mM $K_4[Fe(CN)_6]/K_3[Fe(CN)_6]$ solution.

The pH of the buffer solutions was adjusted using a combined glass electrode (EI 1110, Hanna Instruments) connected to a pH meter (type MV 870, Pracitronic, Germany).

All studies were conducted at room temperature.

Thermogravimetric analysis (TGA) was carried out using a TGA 4000 Perkin Elmer in a temperature range from 25 °C to 850 °C and a ramp rate of 10 °C min^{-1}, under an oxygen flow (flow rate = 40 mL min^{-1}). An X'PERT Pro PANalytical diffractometer was used for X-ray diffraction (XRD) experiments with Cu Kα radiation. The data were collected with a 2θ step size of 0.026 from 5 to 40° and an accumulation time of 20 s. ZIF-8 morphological features were collected via electron microscopy using a Field Emission Gun Scanning Electron Microscope SIGMA (FEG-SEM, Carl Zeiss Microscopy GmbH, Germany), with an acceleration potential of 5 kV and a 6.4 mm working distance. Prior to SEM analysis, dried samples were covered with gold by an Agar Scientific Auto Sputter Coater. The FTIR analysis was performed using a Bruker Tensor 27 spectrophotometer equipped with a diamond-ATR accessory and a DTGS detector. FTIR spectra were carried out by recording 128 scans at a resolution of 2 cm^{-1} in the spectral range 4000–400 cm^{-1}. N_2 adsorption/desorption isotherms were recorded at 77 K using a 3Flex Adsorption Analyzer (Micromeritics). Samples were first degassed under vacuum for 12 h at 25 °C. The Brunauer–Emmett–Teller (BET) and the Barret–Joyner–Halenda (BJH) methods were used to calculate the specific surface area [26], the pore volume, and the pore size distribution [27].

2.3. Preparation of ZIF-8

ZIF-8 was synthesised according to the procedure reported by Wu et al. [28]. Briefly, 4 mL of a $Zn(NO_3)_2$ solution (0.31 M) was added dropwise to 40 mL of a 2-methylimidazole (1.25 M) solution. The reaction mixture was stirred at room temperature for 45 min. Afterwards, the resulting white solid in suspension (ZIF-8) was collected by centrifugation (8000 rpm) and washed three times with Milli-Q water. Finally, the obtained sample was dried for 12 h, at 25 °C, under vacuum.

2.4. Preparation of ZIF-8-rGO-Nafion/GCE modified electrode

The glassy carbon electrode (GCE, from ALS Co., Ltd., inner diameter 3 mm) was polished with alumina powder (0.3 μm, Buehler) to obtain a clean electrode surface. A suspension containing 1 mg of ZIF-8, 1 mg of rGO, 0.5 mL of Nafion of 5 % ethanolic solution and 1 mL of distilled water was sonicated for 20 min in an Elmasonic bath (model S10, Elma, frequency 37 kHz, power 30 W). The presence of distilled water in the suspension has the role of diluting the Nafion ethanolic solution, to obtain a more mechanically resistant and homogeneous polymeric film. Then, the ZIF-8–rGO–Nafion/GCE modified electrode was prepared by the drop-casting method, consisting of dropping 5 μL of previously prepared solution on the electrode surface and waiting 24 h for solvent evaporation, under controlled temperature and pressure conditions.

3. Results and discussion

3.1. Characterisation of ZIF-8

Fig. 1A shows the XRD pattern of the synthesised ZIF-8 MOF. The pattern is well resolved with peaks at $2\theta = 7.4°$, 10.5°, 12.8°, 14.8°,16.6° and 18.2° corresponding to planes (110), (200), (211), (220), (310), and (222) respectively, in agreement with the referenced pattern of the ZIF-8 structure reported in the literature (CCDC 602542) [13,29]. Thermogravimetric analysis of ZIF-8 (Fig. 1B) showed a mass loss of approximately ~20 % at $T < 180$ °C due to the removal of water and unreacted reagents. The ZIF-8 sample is stable up to 360 °C, whilst the mass loss at higher temperatures is ascribed to the decomposition of the material [30]. The ATR-FTIR spectra of ZIF-8 samples are shown in Fig. 1C. The typical peaks at 2928 cm^{-1}, 1584 cm^{-1}, are due to the aromatic and aliphatic C—H asymmetric stretching and the C═N stretching, respectively [31]. The signals between 1300 cm^{-1} and 1460 cm^{-1} are attributed to the ring stretching, whilst the band at 1145 cm^{-1} arise from aromatic C—N stretching mode. Similarly, the peaks at 995 and 760 cm^{-1} could be assigned to the C—N bending and C—H bending modes, respectively. The band at 695 cm^{-1} is due to the out-of-plane bending of the 2-methylimidazole ring. The band at 426 cm^{-1}, assigned to a Zn—N stretching, is due to the coordination of zinc ions with the nitrogen atoms of the methylimidazole groups, confirming the formation of the imidazolate [32]. The Raman spectra of ZIF-8 shown in Fig. 1D exhibited

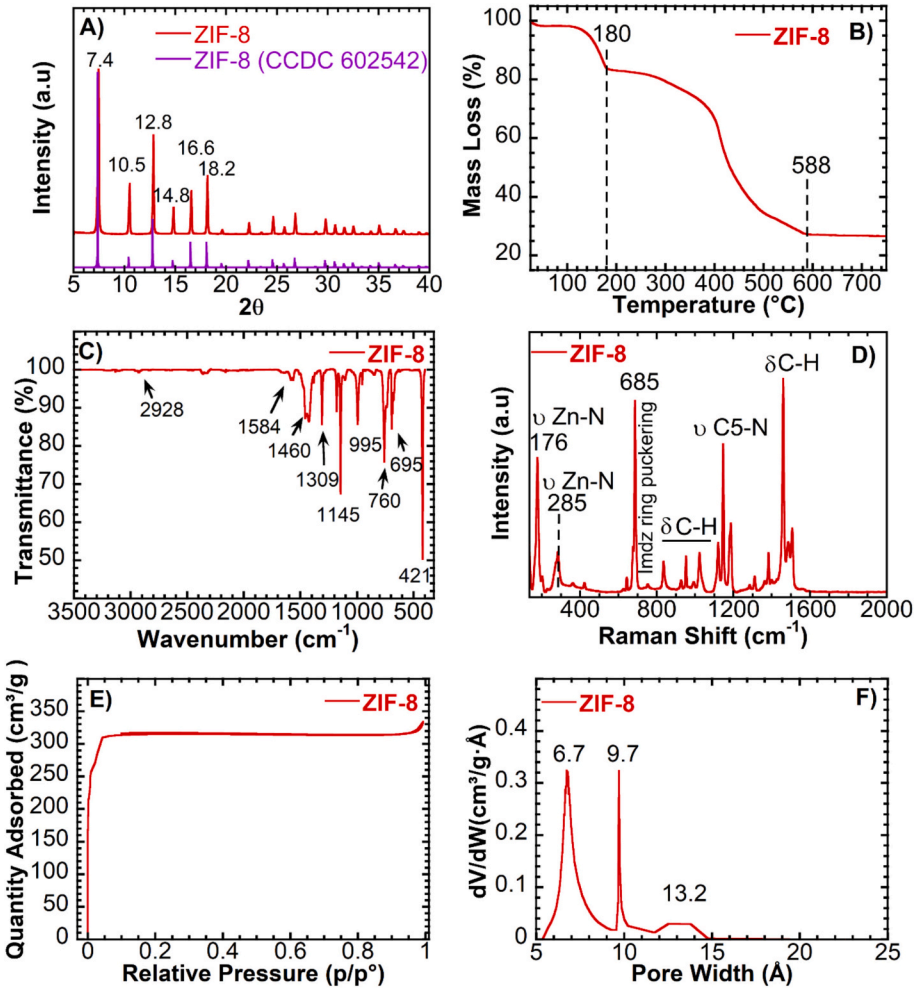

Fig. 1. ZIF-8 characterisation: **A)** XRD patterns of ZIF-8. **B)** Thermogravimetric analysis (TGA) curves from 25 °C to 800 °C of ZIF-8. **C)** FT-IR spectrum of ZIF-8 wavenumber range from 450 to 3600 cm^{-1}. **D)** Raman spectrum of ZIF-8 (wavenumber range from 150 to 2000 cm^{-1}). **E)** N_2 adsorption/desorption isotherms. **F)** pore width distribution of ZIF-8.

sharp bands at 176 cm^{-1}, 685 cm^{-1}, 1145 cm^{-1}, and 1460 cm^{-1} imputable to Zn − N stretching, imidazole ring puckering, C5 − N stretching and methyl bending, respectively [30].

The surface area (S_{BET}), pore volume and pore size distribution of ZIF-8 were also determined through N_2 adsorption−desorption isotherms. A type-I isotherm ((according to the IUPAC classification 1985 [33], typical for microporous materials (Fig. 1E), was obtained. ZIF-8 exhibited a S_{BET} of 1253 $m^2\ g^{-1}$ and a pore volume of 0.512 $cm^3\ g^{-1}$, respectively. The pore size distribution plot (Fig. 1F) showed two sharp peaks at 6.7 Å and 9.7 Å and a broad peak over the range 9–15 Å. Scanning electron microscopy (SEM) images (Fig. 2) of ZIF-8 show the expected rhombic dodecahedron morphology typical of ZIF-8 in SOD phase.

3.2. Electrochemical behaviour of the ZIF-8-rGO-Nafion/GCE modified electrode

In order to estimate the electrochemically active surface of the ZIF-8–rGO–Nafion/GCE modified electrodes, cyclic voltammograms were recorded at the electrode immersed in 0.1 M KCl containing 5 mM $K_4[Fe(CN)_6]/K_3[Fe(CN)_6]$ solution, at different scan rate (Fig. 3A). Then, the graph $I_{pa} - v^{1/2}$ was plotted to be able to use the slope of the Randles-Sevcik eq. (1) for the estimation of the electrode area [34]:

$$I_p = 2.69 \times 10^5 \times n^{3/2} \times A \times D^{1/2} \times C \times v^{1/2} \quad (1)$$

where I_p is the peak current (in A); n is the number of electrons transferred in the redox process (in our case 1); A represents the electrode area (in cm^2); D is the diffusion coefficient (in cm^2/s, in our case $D = 6.5 \times 10^{-6}$ cm^2/s [35]; C is the concentration of the redox species (in mol/cm^3, in our case $C = 5 \times 10^{-6}$ mol/cm^3); ν is the scan rate (in *V*/s).

The corresponding fitted Eqs. (2)–(3) for anodic and cathodic peaks, respectively, are:

$$I_{pa}/A = (1.268 \times 10^{-5} \pm 0.426 \times 10^{-5}) + (3.668 \times 10^{-4} \pm 1.195 \times 10^{-5}) \times v^{1/2}/(V/s)^{1/2}, R^2 = 0.994, n = 8 \text{ points} \quad (2)$$

$$I_{pc}/A = (1.445 \times 10^{-5} \pm 0.493 \times 10^{-5}) + (3.550 \times 10^{-4} \pm 1.384 \times 10^{-5}) \times v^{1/2}/(V/s)^{1/2}, R^2 = 0.991, n = 8 \text{ points} \quad (3)$$

The mean electrode area estimated as the arithmetic mean of anodic and cathodic area was 0.106 ± 0.002 cm^2, which is a value 1.5 times greater than the geometric area of the electrode (for a 3 mm diameter).

In order to assess the changes in the surface characteristics due to the activity of ZIF-8 and rGO immobilised on the surface of ZIF-8–rGO–Nafion/GCE modified electrode, electrochemical impedance spectroscopy (EIS) measurements were performed in a solution containing the redox probe $[Fe(CN)_6]^{4-/3-}$, and represented as Nyquist plots (Fig. 3B). As can be seen, all electrodes present a well-shaped semicircle, characterised by the resistance to the charge transfer (R_{ct}) that flattens in the presence of ZIF-8. The obtained experimental data were fitted by a simple Randles equivalent electric circuit $R_{sol}(Q(R_{ct}W))$ for GCE electrode and by $R_{sol}(Q_{film}(R_{film}(Q_{dl}R_{ct})))$ for all other electrodes. The components of the electric circuits are resistors associated with the resistance of solution (R_{sol}), of charge transfer (R_{ct}), or of the film (R_{film}), constant phase elements (suggesting that the electrode-electrolyte interface works as a non-ideal capacitor) associated with the film (Q_{film},) or with the electrochemical double layer (Q_{dl}), and a Warburg impedance (W). The applicability of the fitted data was verified by the Chi^2 statistical parameter, which is in the range of 10^{-3}.

At bare GCE, the semicircle has a small diameter, indicating the absence of any substance on the electrode surface that blocks the electron transfer (Fig. 3B, inset). When the GCE is modified with Nafion, rGO, or ZIF-8, the diameter of the semicircle increases, indicating a higher R_{ct} value, due to the presence of modifiers on the electrode surfaces. It must be highlighted that the Warburg impedance usually increases at low frequencies, as the reactants must diffuse further through the electrode matrix. However, probably due to the high conductivity of the ZIF-8-rGO-Nafion nanocomposite matrix components, which improves the electron transfer process rate, the diffusion process is no longer visible in the impedance spectra.

Thus, the presence of rGO and ZIF-8 on rGO–Nafion/GCE, ZIF-8–Nafion/GCE and ZIF-8–rGO–Nafion/GCE electrode surfaces improves the conductivity, compared to the poor charge transfer to Nafion/GCE. This observation is supported by the values of the R_{ct}, which decrease in the following order: 6311 kΩ at Nafion/GCE > 1650 kΩ at ZIF-8–Nafion/GCE > 921 kΩ at rGO–Nafion/GCE > 586 kΩ at ZIF-8–rGO–Nafion/GCE > 6.046 kΩ at GCE. The lowest value of charge transfer resistance is associated with an electron transfer process, which occurs more easily at ZIF-8–rGO-Nafion/GCE modified electrode. This behaviour is due to the large surface area induced by the enhanced conductivity of the rGO or/and catalytic activity of ZIF-8 present on the nanocomposite matrix of the electrode [36,37].

3.3. Electrochemical behaviour of the ZIF-8-rGO-Nafion/GCE modified electrode for dopamine detection

The electrochemical behaviour of the 10^{-4} M dopamine at different types of electrodes (i.e., GCE, Nafion–rGO/GCE, ZIF-8–Nafion/GCE, and ZIF-8–rGO–Nafion/GCE) is presented in Fig. 4. As expected, the cyclic voltammograms showed a typical peak pair corresponding to the quasi-reversible redox reaction when ZIF-8 is present in the electrode modifier matrix, as compared with the bare GCE. The following electrochemical parameters are calculated: the peak-to-peak separation (ΔE_p) as the difference between E_{pa} and E_{pc}; the formal potential ($E^{0,}$) as the arithmetic mean of E_{pa} and E_{pc}; and the I_{pa}/I_{pc} ratio. Thus, the estimated ΔE_p, $E^{0,}$ and I_{pa}/I_{pc} values are: +0.452 *V* vs. Ag/AgCl,KCl_{sat}, +0.278 V vs. Ag/AgCl,KCl_{sat} and 0.853 at ZIF-8-Nafion/GCE, and + 0.260 V vs. Ag/AgCl, KCl_{sat},+0.230 V vs. Ag/AgCl,KClsat, and 0.632 at ZIF-8–rGO–Nafion/GCE modified electrode, respectively. At bare GCE, the redox process of dopamine occurs with the following electrochemical parameters: ΔE_p is +0.395 *V* vs. Ag/AgCl,KCl_{sat}, $E^{0,} = 0.322$ V vs. Ag/AgCl,KCl_{sat}, and I_{pa}/I_{pc} ratio of 4.4. This electrochemical behaviour is due to a very low reduction behaviour of dopamine at GCE, which was improved by using

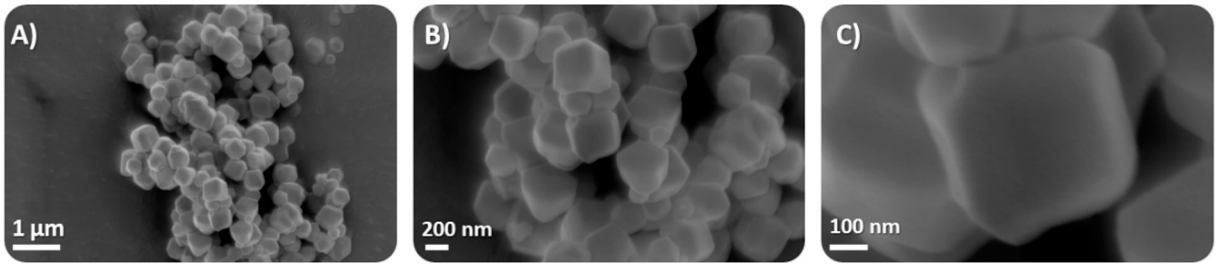

Fig. 2. SEM images of ZIF-8 sample at different magnifications.

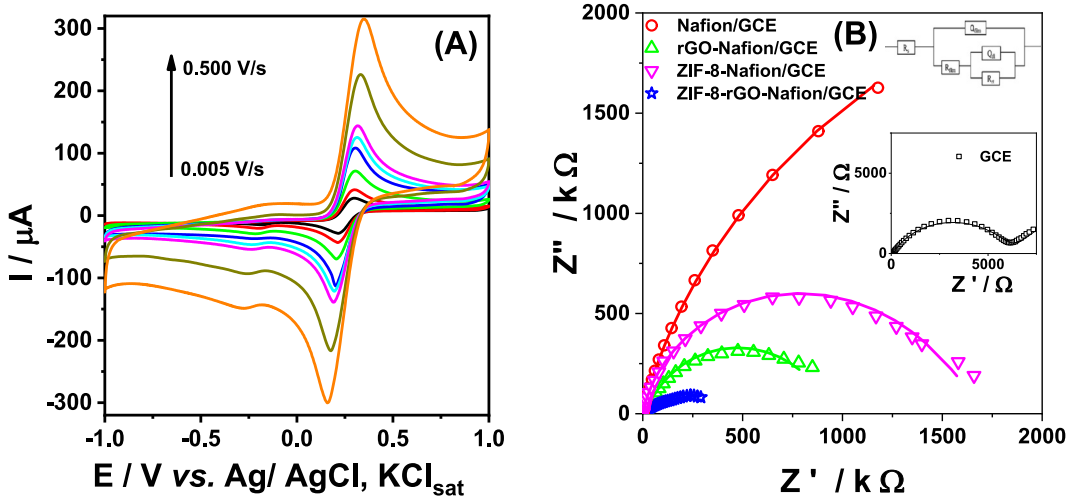

Fig. 3. (A) Influence of the scan rate (see inset) at ZIF-8–rGO–Nafion/GCE modified electrode. (B) Nyquist plots recorded at GCE (□, black, inset), Nafion/GCE (○, red), rGO-Nafion/GCE (Δ, green), ZIF-8–Nafion/GCE (▽, magenta) and ZIF-8–rGO–Nafion/GCE (☆, blue) modified electrodes. Experimental conditions: 0.1 M KCl solution containing 5 mM $K_4[Fe(CN)_6]/K_3[Fe(CN)_6]$ (A, B); scan rate, see inset (A); starting potential, −1 V vs. Ag/AgCl, KCl_{sat} (A), frequency range, 10^{-2}–10^4 Hz (B); amplitude, 10 mV (B); time for OCP measurements, 600 s (B); fitted data (solid lines) (B). (For interpretation of the references to colour in this figure legend, the reader is referred to the web version of this article.)

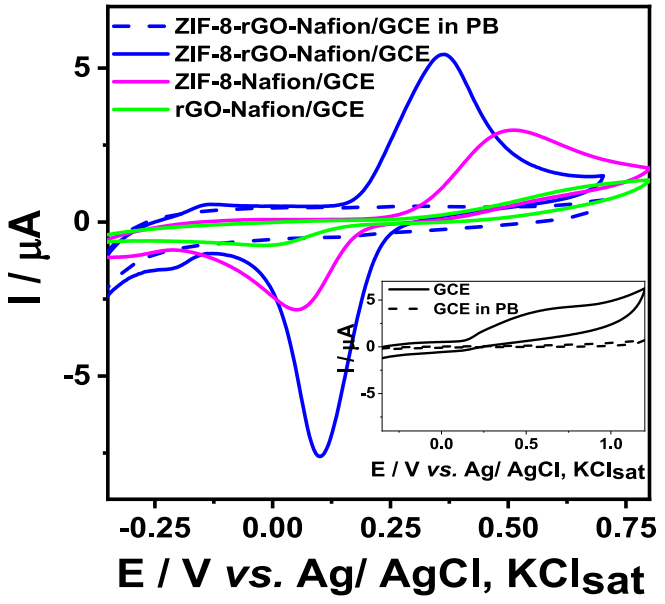

Fig. 4. Cyclic voltammograms at different modified electrodes (see inset): in the absence (dot line, blue or black) and in the presence (solid line, coloured) of 1×10^{-4} M dopamine. Experimental conditions: electrolyte, 0.1 M PB solution (pH 7); scan rate, 0.05 V/s; starting potential −0.4 V vs. Ag/AgCl, KCl_{sat}. (For interpretation of the references to colour in this figure legend, the reader is referred to the web version of this article.)

an appropriate modifier matrix on the electrode interface. Also, the previously mentioned values of the electrochemical parameters estimated in the presence of ZIF-8–rGO showed that the redox process of dopamine is more reversible than in the case when rGO is absent from the electrode matrix.

The possible mechanism of the reactions occurring at the ZIF-8–rGO–Nafion/GCE modified electrode interface may involve: (i) π–π interactions between the planar hexagonal carbon structure of rGO and the benzene rings of dopamine, which leads to an enhance of the adsorption energy and facilitate electron transfer due to the high conductivity of rGO [38]. Also, —OH and —COOH active functional groups existing on the rGO surface act as trapping agents during the catalytic redox reactions involving dopamine; (ii) during the oxidation of dopamine, the two electrons lost are used for the reduction of the Zn^{2+} to Zn from the ZIF-8 structure. Thus, due to the synergetic effect between the high conductivity of the rGO and the catalytic properties of the ZIF-8, the electrons are cycling, and the redox process involving dopamine occurs at the electrode interface.

The kinetics of the redox behaviour of $1 \bullet \times 10^{-4}$ M dopamine at the surface of bare and modified electrodes was investigated by conducting CV experiments at different scan rates between 5 and 500 mV/s. For example, the behaviour of the ZIF-8–rGO–Nafion/GCE modified electrode is presented in Fig. 5A. For all studied electrodes the oxidation/reduction current intensities of the peak pairs increase as the scan rate increases, and their potential shifts slightly at positive and negative values. For all investigated electrodes, the log I - log v dependencies are linear (Fig. 5B), and the slopes are summarized in Table 1. At bare GCE, the dopamine redox behaviour is under diffusion control, with slopes of the log I - log v dependencies around 0.5, with the lowest correlation coefficients. Contrarily, the presence of ZIF-8 at the electrode interface (i.e., ZIF-8–Nafion/GCE modified electrode) induces the partial adsorption of dopamine on the electrode surface, as proven by the slopes placed between 0.5 and 1. At this type of electrode, a mixed diffusion-adsorption controlled oxidation process of dopamine occurs. However, in the presence of rGO (i.e., ZIF-8–rGO–Nafion/GCE modified electrode) the slope decreases at a value of 0.5, suggesting that the redox behaviour of dopamine at the ZIF-8–rGO–Nafion/GCE modified electrode is controlled by diffusion, as described by the Randles Sevcik equation, when I_p is directly proportional with the $v^{1/2}$ [34,39]. The values of the coefficient of determination (R^2) confirm the synergistic positive effect of ZIF-8 and rGO in the electrode matrix, with the highest value observed in the case of the ZIF-8–rGO–Nafion/GCE modified electrode.

The influence of buffer's pH on the redox behaviour of 1×10^{-4} M dopamine was studied on different modified electrodes in the pH range of 6–8. The cyclic voltammogram recorded at ZIF-8–rGO–Nafion/GCE modified electrode (Fig. 6A) shows that the anodic peak potentials are shifted to more negative values, probably because the process of dopamine oxidation is more influenced by the increase of pH value, than the dopamine reduction process, where the peak potential is more stable. The influence of the pH values on the formal potential (calculated as the arithmetic mean of the anodic and cathodic peak potential values) is presented in Fig. 6B. At bare GCE ($E^{0'}/V = (0.502 \pm 0.048) - (0.024 \pm 0.001) \times$ pH, $R^2 = 0.860$, $n = 4$ points), the slope value of 0.024 for the E

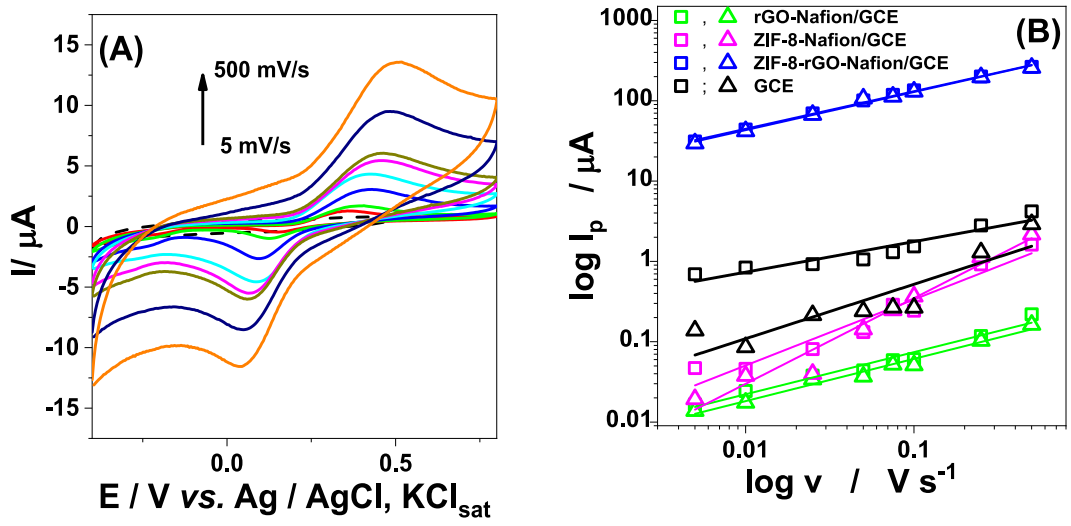

Fig. 5. Influence of the scan rate on the ZIF-8–rGO-Nafion/GCE modified electrode in 1• × 10^{-4} M dopamine (A) and the corresponding log I vs. log v dependence of anodic (□) and cathodic (Δ) process at bare GCE and different modified electrodes (see inset) (B). Experimental conditions: scan rate, see inset (A); starting potential −0.400 *V* vs. Ag/AgCl, KCl_{sat}.

Table 1
Slopes of the log I-log v dependencies at different modified electrodes.

Type of electrode	Anodic process		Cathodic process	
	Slope	R^2 / no. of points	Slope	R^2 / no. of points
GCE	0.381 ± 0.051	0.901 / 8	0.677 ± 0.133	0.811 / 8
Nafion/GCE	0.524 ± 0.038	0.969 / 8	0.526 ± 0.031	0.979 / 8
ZIF-8–Nafion/GCE	0.822 ± 0.083	0.942 / 8	1.067 ± 0.083	0.967 / 8
ZIF-8–rGO–Nafion/GCE	0.468 ± 0.010	0.997 / 8	0.474 ± 0.016	0.993 / 8

– pH dependence means a $1H^+ + 2e^-$ redox process, which can be due to an incomplete redox reaction occurring at this electrode. It must be noticed that the redox behaviour of dopamine is not influenced by the variation of the buffer's pH value at ZIF-8–Nafion/GCE modified electrode (i.e., $E^{o'}$ /*V* = (0.107 ± 0.003) - (0.006 ± 0.001) × 10^{-1} × pH, R^2 = 0.729, *n* = 3 points). Moreover, at ZIF-8–rGO–Nafion/GCE modified electrode, the slope of E – pH dependence is 0.050 ± 0.01 V/pH, close to the theoretic value of 0.059, confirming the slight sub-Nernstian behaviour of dopamine ($E^{o'}$ /V = (0.605 ± 0.010) - (0.050 ± 0.008) × pH, R^2 = 0.922, n = 4 points). This slope value shows that the redox process of dopamine involves $2H^+ + 2e^-$, according to the reaction presented in the literature (see Scheme 1) [25].

In the meantime, the peak current of dopamine oxidation at ZIF-8–rGO–Nafion/GCE modified electrode has the highest value at pH 7.1. That pH value was then used for the following experiments.

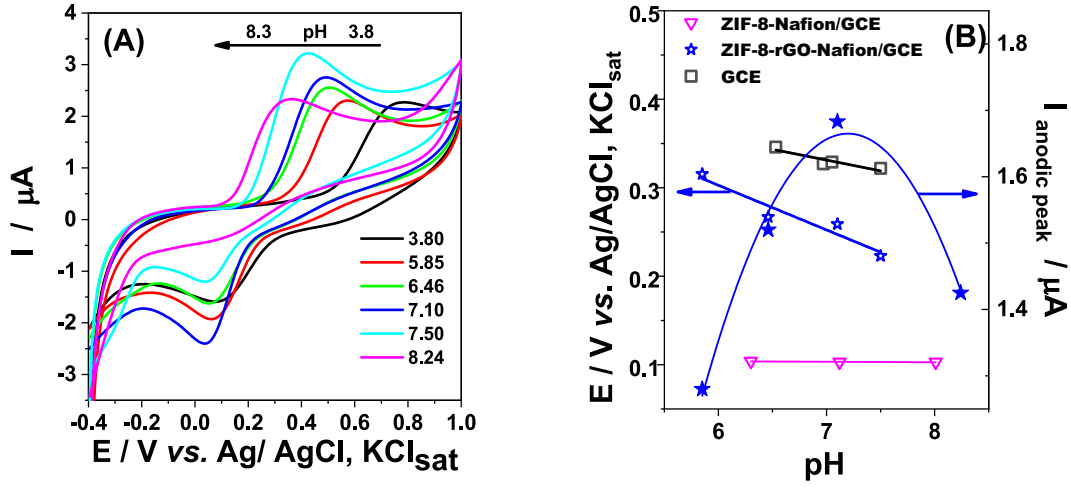

Fig. 6. Influence of the pH on the CVs recorded at ZIF-8-rGO-Nafion/GCE modified electrode in 1 × 10^{-4} M dopamine (A) and the corresponding $E^{o'}$ versus pH and $I_{p,a}$ versus pH dependences at GCE (□, black), ZIF-8-Nafion/GCE (▽, magenta) and ZIF-8-rGO-Nafion/GCE (☆, ★, blue) modified electrode (B). Experimental conditions: electrolyte, 0.1 M PB solution (pH see inset, A); scan rate, 50 mV/s; starting potential −0.4 V vs. Ag/AgCl, KCl_{sat}. (For interpretation of the references to colour in this figure legend, the reader is referred to the web version of this article.)

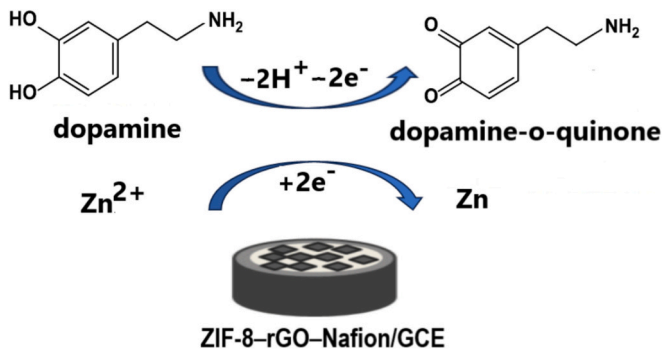

Scheme 1. Reaction of the dopamine reduction [25,38,40–42].

3.4. Analytical performances of the ZIF-8–rGO–Nafion/GCE modified electrode

The electroanalytical performances of the ZIF-8–rGO–Nafion/GCE modified electrode were analysed by conducting square-wave voltammetry experiments for dopamine quantitative determination. Fig. 7A shows the increase in peak current intensity when the concentration of dopamine is increased. The corresponding calibration curves show a linear domain in the range of 0.5–1.4 μM (Fig. 7B), described by the following Eqs. (4)–(7):

$$I_p/A = (-0.880 \pm 0.231) \times 10^{-7} + (0.444 \pm 0.023) \times [\text{dopamine}]/M, R^2 = 0.979, n = 10 \text{ points, at GCE;} \quad (4)$$

$$I_p/A = (-0.227 \pm 0.046) \times 10^{-7} + (0.074 \pm 0.005) \times [\text{dopamine}]/M, R^2 = 0.969, n = 11 \text{ points, at rGO–Nafion/GCE;} \quad (5)$$

$$I_p/A = (0.193 \pm 0.041) \times 10^{-7} + (0.093 \pm 0.004) \times [\text{dopamine}]/M, R^2 = 0.985, n = 11 \text{ points, at ZIF} - 8\text{–Nafion/GCE;} \quad (6)$$

$$I_p/A = (-7.149 \pm 0.103) \times 10^{-7} + (0.590 \pm 0.010) \times [\text{dopamine}]/M, R^2 = 0.998, n = 10 \text{ points, at ZIF} - 8\text{–rGO–Nafion/GCE.} \quad (7)$$

The sensitivity of the bare GCE electrode and all modified types of electrodes decreases in the order: 0.590 A/M (at ZIF-8–rGO–Nafion/GCE) > 0.444 A/M (at GCE) > 0.093 A/M (at ZIF-8–Nafion/GCE) > 0.074 A/M (at rGO–Nafion/GCE), with the highest value for the modified ZIF-8–rGO–Nafion/GCE electrode. This behaviour shows that for the redox process of dopamine occurring at the modified electrode, (i) the presence of only the highly conductive rGO is not enough if the catalyst (i.e. ZIF-8) is absent, and (ii) the presence of both rGO and ZIF-8 has a synergistic effect that leads to an increase of 6 times of the sensitivity of the detection.

The limit of detection, calculated as LOD = 3 × s_A/ b (where: s_A is the standard deviation of the intercept from the calibration curve equation and b is the slope of the calibration curve), decreases in the following order at rGO–Nafion/GCE (0.187 μM) > GCE (0.156 μM) > ZIF-8–Nafion/GCE (0.130 μM) > ZIF-8–rGO–Nafion/GCE (0.051 μM) modified electrode, respectively, proving the beneficial effect of the rGO and ZIF-8 in the modified matrix of the electrode.

In real samples, dopamine, paracetamol and citric acid can coexist with quasi-similar redox potentials. This is the reason for evaluating the simultaneous detection of these analytes with the modified ZIF-8–rGO–Nafion/GCE electrode. As seen in Fig. 8A, the peak potentials placed at −0.050, +0.250, and + 0.470 *V* vs. Ag/AgCl, KCl_{sat} correspond to the oxidation of paracetamol, dopamine and citric acid, respectively. Thus, the peak of dopamine oxidation is visibly well-separated from the peak of paracetamol oxidation, while the peak of citric acid appears at a more positive value of potential, with a reduced intensity current, which probably makes its detection harder to realise. However, a peak potential separation of more than 0.2 V could be advantageous to the simultaneous determination of these analytes, without interference. The linear regression eqs. (8–10) for the studied analytes are:

$$I_p/A = (-1.649 \pm 0.006) \times 10^{-7} + (0.610 \pm 0.008) \times [\text{Dopamine}]/M, R^2 = 0.998, n = 10 \text{ points} \quad (8)$$

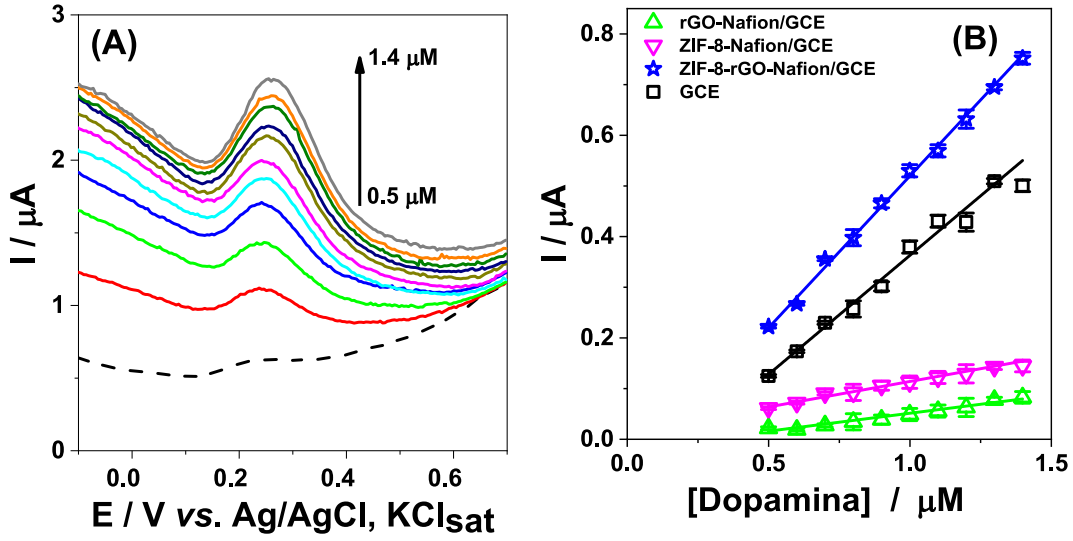

Fig. 7. SW*V* at ZIF-8–rGO–Nafion/GCE modified electrode in the absence (dot line, black) and in the presence of different concentrations of dopamine (solid lines, coloured) (A) and the corresponding calibration curves (B). Experimental conditions: electrolyte, 0.1 M PB solution (pH 7.1); frequency, 10 Hz; amplitude, 0.05 V; step potential, 0.0045 V, starting potential, −0.4 V vs. Ag/AgCl,KCl_{sat}; analyte stock solution, 10^{-4} M dopamine.

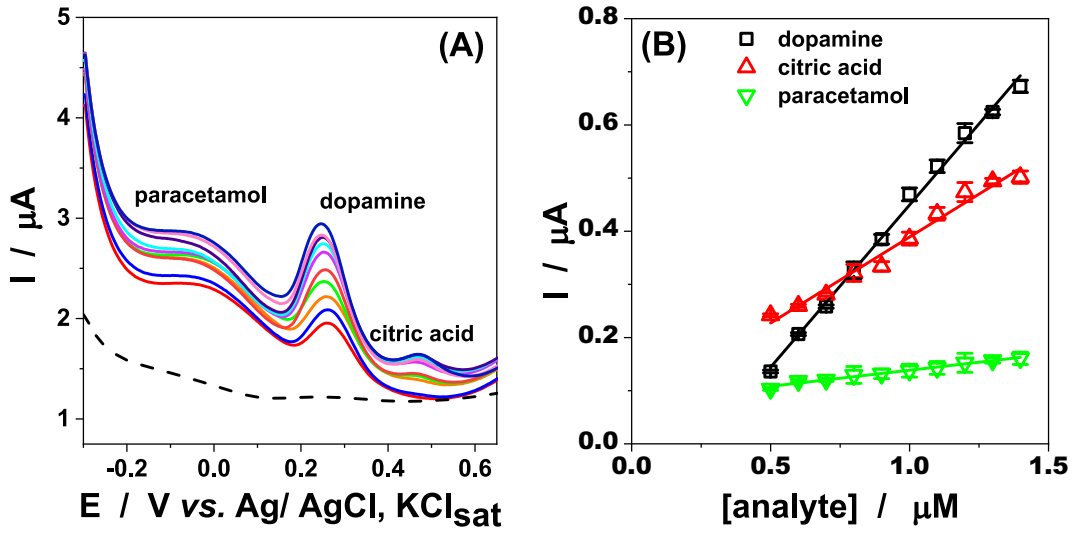

Fig. 8. SWV voltammograms for simultaneous detection of dopamine (□, black), citric acid (Δ, red), and paracetamol (▽, green) at ZIF-8–rGO–Nafion/GCE modified electrode (A) and the corresponding calibration curves (B). Experimental conditions: electrolyte, 0.1 M PB solution (pH 7.1); frequency, 10 Hz; amplitude, 0.05 V; step potential, 0.0045 V; starting potential −0.4 V vs. Ag/AgCl,KCl_{sat}. (For interpretation of the references to colour in this figure legend, the reader is referred to the web version of this article.)

$$I_p/A = (6.574 \pm 1.618) \times 10^{-8} + (0.324 \pm 0.016) \times [\text{Citric acid}]/M, R^2 = 0.980, n = 10 \text{ points} \quad (9)$$

$$I_p/A = (7.816 \pm 0.300) \times 10^{-8} + (0.061 \pm 0.003) \times [\text{Paracetamol}]/M, R^2 = 0.980, n = 10 \text{ points} \quad (10)$$

The LOD vary in the following order: 0.069 µM dopamine <0.148 µM for paracetamol ≈ 0.149 µM citric acid.

A possible explanation for these good analytical sensing performances is (i) the porous structure of the ZIF-8 matrix that could allow easy access of analyte molecules to the electrode surface and consequently promote the electrooxidation process (corroborate with BET analysis) and (ii) the combination with highly electric conductive reduced graphene oxide (rGO) that could compensate the limited electrical conductivity of ZIF-8 and consequently enhance the electrochemical activity of the proposed modified electrode matrix (corroborate with EIS measurements) [23].

From Table 2, it can be observed that, in contrast with the previously reported modified electrodes, the proposed ZIF-8–rGO–Nafion/GCE modified electrodes have a linear enough concentration range for dopamine detection with a lower detection limit. Even if different graphene derivatives were used in the electrode matrix, and even if the linear ranges were larger, the reported limits of detection were not significantly lower.

The reproducibility of the ZIF-8–rGO–Nafion/GCE modified electrode was explored by measuring the corresponding peak current intensity in a 0.5 µM dopamine solution using three different electrodes prepared in the same conditions. The average peak current intensity value was (5.856 ± 0.446) × 10^{-7} A (RSD = 7.43 %) and the peak potential 0.250 ± 0.002 V (RSD = 0.92 %).

Also, the repeatability of four measurements performed with the same electrode led to an average value of the peak potential of (0.277 ± 0.008) *V* (RSD = 2.70 %), and of peak current intensity of (1.846 ± 0.032) × 10^{-7} A (RSD = 1.72 %), respectively. These results suggest that the ZIF-8–rGO–Nafion/GCE modified electrode had good reproducibility and repeatability.

Cyclic voltammetry was used to study the electrode's short-term stability during 25 cycles (results not shown). After 15 min of tests, the anodic and cathodic peak intensities decreased by less than 5 %, indicating that the modified electrode is stable during operation.

Selectivity is an important parameter for characterising a new electrochemical sensor from an analytical point of view. As coexistent substances, citric acid (CA), paracetamol (Pa), glucose, KCl, NaCl and their mixture were selected for this study. In a typical SWV experiment, the

Table 2
Comparison of the analytical parameters of ZIF-8–rGO–Nafion/GCE modified electrode with other reported electrodes for dopamine detection.

Type of electrode	Method of investigation	Linear domain/ µM	LOD/ µM	References
GO-Y_2O_3/GCE	SWV	0.5–350	0.05	[25]
Graphene–ZIF-8/GCE	CV	3–1000	1	[22]
ZIF-8–Nafion/GCE	DPV	0.05–0.5/1.0–20.0	0.195/0.529	[43]
IL–rGO /ZIF-8/GCE	DPV	0.1–100	0.035	[44]
Au@ZIF-8 NP/GCE	DPV	0.1–50	0.01	[45]
ZnS–Sb_2S_3/C/ GCE	DPV	0.21–3.11 3.11–710	0.6	[46]
rGO–Nafion/GCE	SWV	0.5–1.4	0.187	This work
ZIF-8–Nafion/GCE	SWV	0.5–1.4	0.130	This work
ZIF-8–rGO - Nafion/GCE	SWV	0.5–1.4	0.051	This work
ZIF-8–rGO - Nafion/GCE	SWV*	0.5–1.4	0.069 µM dopamine; 0.148 µM for paracetamol; 0.149 µM citric acid	This work

Where: GO = graphene oxide, IL–rGO = ionic-liquid functionalized reduced graphene oxide, Au@ZIF-8 NP = gold nanoparticles and zeolitic imidazolate framework-8 nanoparticles, ZnS–Sb_2S_3/C = carbon coating ZnS-Sb_2S_3 nanocomposite, * as analyte dopamine, paracetamol, citric acid simultaneous.

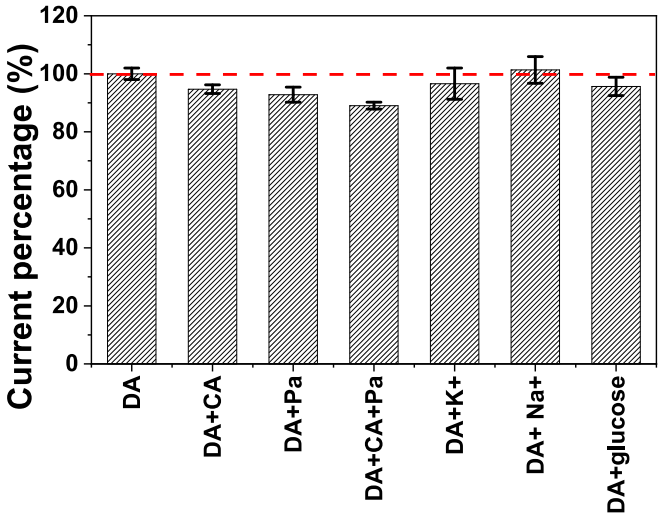

Fig. 9. Current peak intensities of SWV curves at ZIF-8–rGO–Nafion/GCE modified electrode in the presence of 0.1 μM dopamine and 10 μM interferences. Experimental conditions: electrolyte, 0.1 M PB solution (pH 7.1); frequency, 10 Hz; amplitude, 0.05 V; step potential, 0.0045 V; starting potential 0.4 V vs. Ag/AgCl,KCl_{sat}; analytes, dopamine (DA), citric acid (CA), paracetamol (Pa), NaCl (Na+), KCl (K+), glucose.

current peak intensity recorded in the presence of 0.1 μM DA was measured and noted as the standard value (100 %).

Also, the current peak intensities recorded in 0.1 μM dopamine in the presence of a 100-fold excess of interferences (i.e., of 10 μM) were measured, and the ratio $I_{DA+interference}/I_{DA}$ (%) was calculated and compared with the previous value (Fig. 9).

As seen from Fig. 9, compared with the DA in the absence of interference substances, in the presence of all studied interference substances (excepting the case of NaCl), the peak current intensity of DA decreases with a maximum of 11 % (in the case of citric acid + paracetamol), with a relative standard deviation no higher than 5.4 % (in the case of DA + KCl). All these results revealed that the developed ZIF-8–rGO–Nafion/GCE modified electrode has a satisfactory selectivity for the determination of dopamine, in not very complicated real samples.

3.5. Real sample analysis

In order to demonstrate the practical application of the developed electrode, the determination of dopamine in injection vials was tested. For this purpose, the SWV voltammograms were recorded by applying the standard addition method, and the obtained results are summarized in Table 3.

Recoveries, ranging from 110.8 % to 112.6 %, are probably due to the presence of a small amount of maleic acid that could be adsorbed and oxidised at the electrode matrix [47]. However, the recovery values less than 120 % are acceptable in the pharmaceutical industry [48], so it can be concluded that the developed ZIF-8–rGO–Nafion/GCE modified electrode reveals the effectiveness and reliability in the analysis of real samples.

Table 3
Results of real sample analysis by the standard addition method.

Sample	$[DA]_{add}$ / μM	$[DA]_{found}$ / μM	Recovery / %
1	0.500	0.554	110.8
2	0.500	0.559	111.8
3	0.500	0.563	112.6
mean	0.500	0.558 ± 0.003	111,7

4. Conclusions

Previously published research used various modifier materials consisting of graphene or graphene oxide materials decorated with ZIF compounds, by a chemical step [22,25]. Contrarily, this work employed a simple way to prepare a composite solution containing ZIF-8 material, rGO and Nafion ethanolic solution. After that, the glassy carbon-modified electrode (i.e., ZIF-8–rGO–Nafion/GCE) was prepared by the drop-casting method and tested for dopamine detection.

The influence of the scan rate and buffer's pH on the dopamine oxidation process was studied by cyclic voltammetry, leading to the estimation of different electrochemical parameters. By SWV, good electroanalytical performances for separate and simultaneous DA detection were obtained. This could be a favourable approach for developing highly sensitive electrochemical devices. Compared with similar reported data in the literature, the prepared modified electrode demonstrates a synergistic effect of the high conductivity of the reduced graphene oxide (rGO) and the high electroactive surface area of the combined ZIF-8 and rGO presented in the electrode matrix leading to performant analytical parameters for the detection of dopamine in synthetic or real samples.

CRediT authorship contribution statement

Alexandra Belcovici: Writing – original draft, Software, Methodology, Investigation, Data curation, Conceptualization. **Davide Tocco:** Writing – original draft, Validation, Software, Methodology, Investigation, Data curation, Conceptualization. **Emiliano Fratini:** Validation, Supervision, Resources, Funding acquisition. **Andrea Salis:** Writing – review & editing, Writing – original draft, Validation, Supervision, Methodology, Funding acquisition, Formal analysis, Data curation, Conceptualization. **Graziella Liana Turdean:** Writing – review & editing, Writing – original draft, Validation, Supervision, Software, Methodology, Formal analysis, Data curation, Conceptualization.

Declaration of competing interest

The authors declare that they have no known competing financial interests or personal relationships that could have appeared to influence the work reported in this paper.

Acknowledgements

Fondazione di Sardegna (F72F20000230007) and Consorzio Interuniversitario per i Sistemi a Grande Interfase (CSGI, Florence) are acknowledged for support.

Data availability

All relevant data is included in the paper. The experimental data are available on request.

References

[1] S.R. Batten, N.R. Champness, X.-M. Chen, J. Garcia-Martinez, S. Kitagawa, L. Öhrström, M. O'Keeffe, M.P. Suh, J. Reedijk, Coordination polymers, metal–organic frameworks and the need for terminology guidelines, Cryst. Eng. Commun. 14 (2012) 3001, https://doi.org/10.1039/c2ce06488j.
[2] V.V. Butova, M.A. Soldatov, A.A. Guda, K.A. Lomachenko, C. Lamberti, Metal-organic frameworks: structure, properties, methods of synthesis and characterization, Russ. Chem. Rev. 85 (2016) 280–307, https://doi.org/10.1070/RCR4554.
[3] R.L. Siegelman, J.A. Thompson, J.A. Mason, T.M. McDonald, J.R. Long, A cooperative adsorbent for the switch-like capture of carbon dioxide from crude natural gas, Chem. Sci. 13 (2022) 11772–11784, https://doi.org/10.1039/D2SC03570G.
[4] K. Hemmer, M. Cokoja, R.A. Fischer, Exploitation of intrinsic confinement effects of MOFs in catalysis, Chem. Cat. Chem. 13 (2021) 1683–1691, https://doi.org/10.1002/cctc.202001606.

[5] P. Samanta, S. Let, W. Mandal, S. Dutta, S.K. Ghosh, Luminescent metal–organic frameworks (LMOFs) as potential probes for the recognition of cationic water pollutants, Inorg. Chem. Front. 7 (2020) 1801–1821, https://doi.org/10.1039/D0QI00167H.

[6] M.-X. Wu, Y.-W. Yang, Metal-organic framework (MOF)-based drug/cargo delivery and Cancer therapy, Adv. Mater. 29 (2017) 1606134, https://doi.org/10.1002/adma.201606134.

[7] S. Sağlam, F.N. Türk, H. Arslanoğlu, Use and applications of metal-organic frameworks (MOF) in dye adsorption: review, J. Environ. Chem. Eng. 11 (2023) 110568, https://doi.org/10.1016/j.jece.2023.110568.

[8] G.R. Delpiano, D. Tocco, L. Medda, E. Magner, A. Salis, Adsorption of malachite green and alizarin red S dyes using Fe-BTC metal organic framework as adsorbent, Int. J. Mol. Sci. 22 (2021) 788, https://doi.org/10.3390/ijms22020788.

[9] D. Tocco, C. Carucci, D. Todde, K. Shortall, F. Otero, E. Sanjust, E. Magner, A. Salis, Enzyme immobilization on metal organic frameworks: Laccase from Aspergillus sp. is better adapted to ZIF-zni rather than Fe-BTC, Colloids Surf. B: Biointerfaces 208 (2021) 112147, https://doi.org/10.1016/j.colsurfb.2021.112147.

[10] D. Tocco, M. Joshi, R. Mastrangelo, E. Fratini, A. Salis, M. Hartmann, A green approach to encapsulate proteins and enzymes within crystalline lanthanide-based Tb and Gd MOFs, Dalton Trans. 53 (2024) 14171–14181, https://doi.org/10.1039/D4DT01667J.

[11] Q. Ma, T. Zhang, B. Wang, Shaping of metal-organic frameworks, a critical step toward industrial applications, Materials 5 (2022) 1070–1091, https://doi.org/10.1016/j.matt.2022.02.014.

[12] Y. Liu, H. Pang, X. Wang, S. Yu, Z. Chen, P. Zhang, L. Chen, G. Song, N. Saleh Alharbi, S. Omar Rabah, X. Wang, Zeolitic imidazolate framework-based nanomaterials for the capture of heavy metal ions and radionuclides: a review, Chem. Eng. J. 406 (2021) 127139, https://doi.org/10.1016/j.cej.2020.127139.

[13] K.S. Park, Z. Ni, A.P. Côté, J.Y. Choi, R. Huang, F.J. Uribe-Romo, H.K. Chae, M. O'Keeffe, O.M. Yaghi, Exceptional chemical and thermal stability of zeolitic imidazolate frameworks, Proc. Natl. Acad. Sci. USA 103 (2006) 10186–10191, https://doi.org/10.1073/pnas.0602439103.

[14] D. Tocco, D. Wisser, M. Fischer, W. Schwieger, A. Salis, M. Hartmann, Immobilization of Aspergillus sp. laccase on hierarchical silica MFI zeolite with embedded macropores, Colloids Surf. B: Biointerfaces 226 (2023) 113311, https://doi.org/10.1016/j.colsurfb.2023.113311.

[15] D.M. Polyukhov, A.S. Poryvaev, S.A. Gromilov, M.V. Fedin, Precise measurement and controlled tuning of effective window sizes in ZIF-8 framework for efficient separation of xylenes, Nano Lett. 19 (2019) 6506–6510, https://doi.org/10.1021/acs.nanolett.9b02730.

[16] Y. Wang, B. Chen, Y. Zhang, L. Fu, Y. Zhu, L. Zhang, Y. Wu, ZIF-8@MWCNT-derived carbon composite as electrode of high performance for supercapacitor, Electrochim. Acta 213 (2016) 260–269, https://doi.org/10.1016/j.electacta.2016.07.019.

[17] I. Imae, Reduction of graphene oxide using an environmentally friendly method and its application to energy-related materials, Coatings 11 (3) (2021) 297, https://doi.org/10.3390/coatings11030297.

[18] A. Razaq, F. Bibi, X. Zheng, R. Papadakis, S.H.M. Jafri, H. Li, Review on graphene-, graphene oxide-, reduced graphene oxide-based flexible composites: from fabrication to applications, Materials 15 (2022), https://doi.org/10.3390/ma15031012, 1012.

[19] I. Bychko, A. Abakumov, O. Didenko, M. Chen, J. Tang, P. Strizhak, Differences in the structure and functionalities of graphene oxide and reduced graphene oxide obtained from graphite with various degrees of graphitization, J. Phys. Chem. Solids 164 (2022) 110614, https://doi.org/10.1016/j.jpcs.2022.110614.

[20] G. Yu, J. Xia, F. Zhang, Z. Wang, Hierarchical and hybrid RGO/ZIF-8 nanocomposite as electrochemical sensor for ultrasensitive determination of dopamine, J. Electroanal. Chem. 801 (2017) 496–502, https://doi.org/10.1016/j.jelechem.2017.08.038.

[21] S. Ren, J. Zeng, Z. Zheng, H. Shi, Perspective and application of modified electrode material technology in electrochemical voltammetric sensors for analysis and detection of illicit drugs, Sens. Actuat. A: Phys. 329 (2021) 112821, https://doi.org/10.1016/j.sna.2021.112821.

[22] Y.Y. Zheng, C.X. Li, X.T. Ding, Q. Yang, Y.M. Qi, H.M. Zhang, L.T. Qu, Detection of dopamine at graphene-ZIF-8 nanocomposite modified electrode, Chin. Chem. Lett. 28 (2017) 1473–1478, https://doi.org/10.1016/j.cclet.2017.03.014.

[23] M.W. Ahmad, B. Dey, B.H. Kim, G. Sarkhel, D.J. Yang, S.K. Safdar Hossain, T. Kamal, A. Choudhury, Bimetallic copper-cobalt MOFs anchored carbon nanofibers hybrid mat based electrode for simultaneous determination of dopamine and tyramine, Microchem. J. 193 (2023) 109074, https://doi.org/10.1016/j.microc.2023.109074.

[24] A. Karim, M. Yasser, A. Ahmad, H. Natsir, A. Wahid Wahab, St. Fauziah, P. Taba, I. Pratama, A. Rajab Rosalin, A.N.F. Abubakar, T.W. Putri, R. Munadi, A.F. Majid, A. Nur, A. Rifai Fadliah, M. Syahrir, A review: Progress and trend advantage of dopamine electrochemical sensor, J. Electroanal. Chem. 959 (2024) 118157, https://doi.org/10.1016/j.jelechem.2024.118157.

[25] G.S. Shyam Sunder, A. Rohanifar, A.M. Devasurendra, J.R. Kirchhoff, Selective determination of - DOPA at a graphene oxide/yttrium oxide modified glassy carbon electrode, Electrochim. Acta 301 (2019) 192–199, https://doi.org/10.1016/j.electacta.2019.01.098.

[26] S. Brunauer, P. H. Emmett, E. Teller, Adsorption of gases in multimolecular layers, J. Am. Chem. Soc. 60 (1938) 309–319. Doi: citeulike-article-id:4074706\rdoi: https://doi.org/10.1021/ja01269a023.

[27] E.P. Barrett, L.G. Joyner, P.P. Halenda, The determination of pore volume and area distributions in porous substances. I. Computations from nitrogen isotherms, J. Am. Chem. Soc. 73 (1951) 373–380, https://doi.org/10.1021/ja01145a126.

[28] X. Wu, J. Ge, C. Yang, M. Hou, Z. Liu, Facile synthesis of multiple enzyme-containing metal–organic frameworks in a biomolecule-friendly environment, Chem. Commun. 51 (2015) 13408–13411, https://doi.org/10.1039/C5CC05136C.

[29] N.A.H.M. Nordin, A.F. Ismail, N. Misdan, N.A.M. Nazri, Modified ZIF-8 mixed matrix membrane for CO2/CH4 separation, in: AIP Conf. Proc., 2017, https://doi.org/10.1063/1.5005424, p. 020091.

[30] D. Tocco, D. Chelazzi, R. Mastrangelo, A. Casini, A. Salis, E. Fratini, P. Baglioni, Conformational changes and location of BSA upon immobilization on zeolitic imidazolate frameworks, J. Colloid Interface Sci. 641 (2023) 685–694, https://doi.org/10.1016/j.jcis.2023.03.107.

[31] F. Pitzalis, C. Carucci, M. Naseri, L. Fotouhi, E. Magner, A. Salis, Lipase encapsulation onto ZIF-8: a comparison between biocatalysts obtained at low and high zinc/2-Methylimidazole molar ratio in aqueous medium, ChemCatChem 10 (2018) 1578–1585, https://doi.org/10.1002/cctc.201701984.

[32] Y. Zhang, Y. Jia, M. Li, L. Hou, Influence of the 2-methylimidazole/zinc nitrate hexahydrate molar ratio on the synthesis of zeolitic imidazolate framework-8 crystals at room temperature, Sci. Rep. 8 (2018) 1–7, https://doi.org/10.1038/s41598-018-28015-7.

[33] C.I. Fort, L.C. Cotet, F. Vasiliu, P. Marginean, V. Danciu, I.C. Popescu, Methanol oxidation at carbon paste electrodes modified with (Pt-Ru)/carbon aerogels nanocomposites, Mater. Chem. Phys. 172 (2016) 179–188, https://doi.org/10.1016/j.matchemphys.2016.01.06.

[34] C.M.A. Brett, A.M.O. Brett, Electrochemistry: Principles, Methods, and Applications, 1993rd ed., Oxford University Press, 1993.

[35] J.-S. Ye, Y. Wen, W. De Zhang, H.-F. Cui, L. Ming Gan, G. Qin Xu, F.-S. Sheu, Application of multi-walled carbon nanotubes functionalized with hemin for oxygen detection in neutral solution, J. Electroanal. Chem. 562 (2004) 241–246, https://doi.org/10.1016/j.jelechem.2003.09.007.

[36] T.T. Hien Ngo, I.C. Fort, T.H. Pham, G.L. Turdean, Ordered mesoporous silica incorporating platinum nanoparticles as electrode material for paracetamol detection, Electroanalysis 33 (2021) 323–335, https://doi.org/10.1002/elan.202060131.

[37] A. Belcovici, C.I. Fort, L.E. Mureşan, I. Perhaiţa, G. Borodi, G.L. Turdean, Zinc oxide nanostructured platform for electrochemical detection of heavy metals, Electroanalysis 35 (2023) e202200395, https://doi.org/10.1002/elan.202200395.

[38] Y. Li, F. Ren, J. Li, Y. Chen, J. Liu, C. Yang, 1D/2D SnO_2/rGO composites-modified GCE for highly sensitive nonenzymatic electrochemical determination of chloramphenicol, J. Alloys Compd. 1014 (2025) 178637, https://doi.org/10.1016/j.jallcom.2025.178637.

[39] A.J. Bard, L.R. Faulkner, Electrochemical Methods, Wiley-VCH, New York, 2002, p. 522.

[40] B. Wu, L. Xiao, M. Zhang, C. Yang, Q. Li, G. Li, Q. He, J. Liu, Facile synthesis of dendritic-like CeO_2/rGO composite and application for detection of uric acid and tryptophan simultaneously, J. Solid St. Chem. 296 (2021) 122023, https://doi.org/10.1016/j.jssc.2021.122023.

[41] S. Zhang, P. Ling, Y. Chen, J. Liu, C. Yang, 2D/2D porous Co_3O_4/rGO nanosheets act as an electrochemical sensor for voltammetric tryptophan detection, Diam. Relat. Mater. 135 (2023) 109811, https://doi.org/10.1016/j.diamond.2023.109811.

[42] Y. Ding, X. Zhao, P. Wu, R. Wang, L. Xie, Z. Li, Z. Zhu, H. Zhao, M. Lan, ZIF-67 MOF derived co-based CeO_2 electrochemical sensor for dopamine, Electrochim. Acta 463 (2023) 142802, https://doi.org/10.1016/j.electacta.2023.142802.

[43] M. Nie, S. Lu, D. Lei, C. Yang, Z. Zhao, Rapid synthesis of ZIF-8 nanocrystals for electrochemical detection of dopamine, J. Electrochem. Soc. 164 (2017) H952–H957, https://doi.org/10.1149/2.1521713jes.

[44] L. Cheng, Y. Fan, X. Shen, H. Liang, Highly sensitive detection of dopamine at ionic liquid functionalized RGO/ZIF-8 nanocomposite-modified electrode, J. Nanomater. 2019 (2019), https://doi.org/10.1155/2019/8936095.

[45] S. Lu, M. Hummel, K. Chen, Y. Zhou, S. Kang, Z. Gu, Synthesis of au@ZIF-8 nanocomposites for enhanced electrochemical detection of dopamine, Electrochem. Commun. 114 (2020) 106715, https://doi.org/10.1016/j.elecom.2020.106715.

[46] L. Gao, J. Zheng, ZIF-8 supported Sb_2S_3 fabrication carbon coating nanocomposite for dopamine sensor application, Microchem. J. 171 (2021) 106782, https://doi.org/10.1016/j.microc.2021.106782.

[47] F. Epron, M.J. Chollier-Brym, E. Lamy-Pitara, J. Barbier, Oxidation of maleic acid under control of the catalyst potential in a pressurized electrochemical reactor, Appl. Catal. A Gen. 176 (1999) 221–228, https://doi.org/10.1016/S0926-860X(98)00240-3.

[48] E.A. Schoenau, Elements of method design, in: E.A. Schoenau, T. Geng, R. Hill, N. L. Houston, M. Saha, X. Zhou (Eds.), Current Challenges and Advancements in Residue Analytical Methods, ACS Symposium Series; American Chemical Society, Washington, DC, 2019, p. 6.